

Fracture Mechanics of Concrete Structures,
Proceedings FRAMCOS-2, edited by Folker H. Wittmann,
AEDIFICATIO Publishers, D-79104 Freiburg (1995)

SPLITTING OF CONCRETE COVERS - A FRACTURE MECHANICS APPROACH

K. Noghabai

Division of Structural Engineering, Luleå University of Technology
Luleå, Sweden

Abstract

The splitting capacity of concrete cylinders subjected to an inner pressure are investigated experimentally, theoretically and numerically. Three types of concrete are tested: Normal, high and very high strength concrete, (NSC, HSC and VHSC with a compressive strength of 57, 105 and 157 MPa respectively). Reference cylinders with no confining spiral reinforcement are compared to cylinders including a spiral. Two analytical models based on non linear fracture mechanics (NLFM) are evaluated. A good correspondence is observed. Finite element (FE) analysis are successfully performed based on the discrete crack, the smeared crack and the inner softening band (ISB) concepts. The fracturing behaviour of a cylinder is very adequately captured specially by the ISB approach.

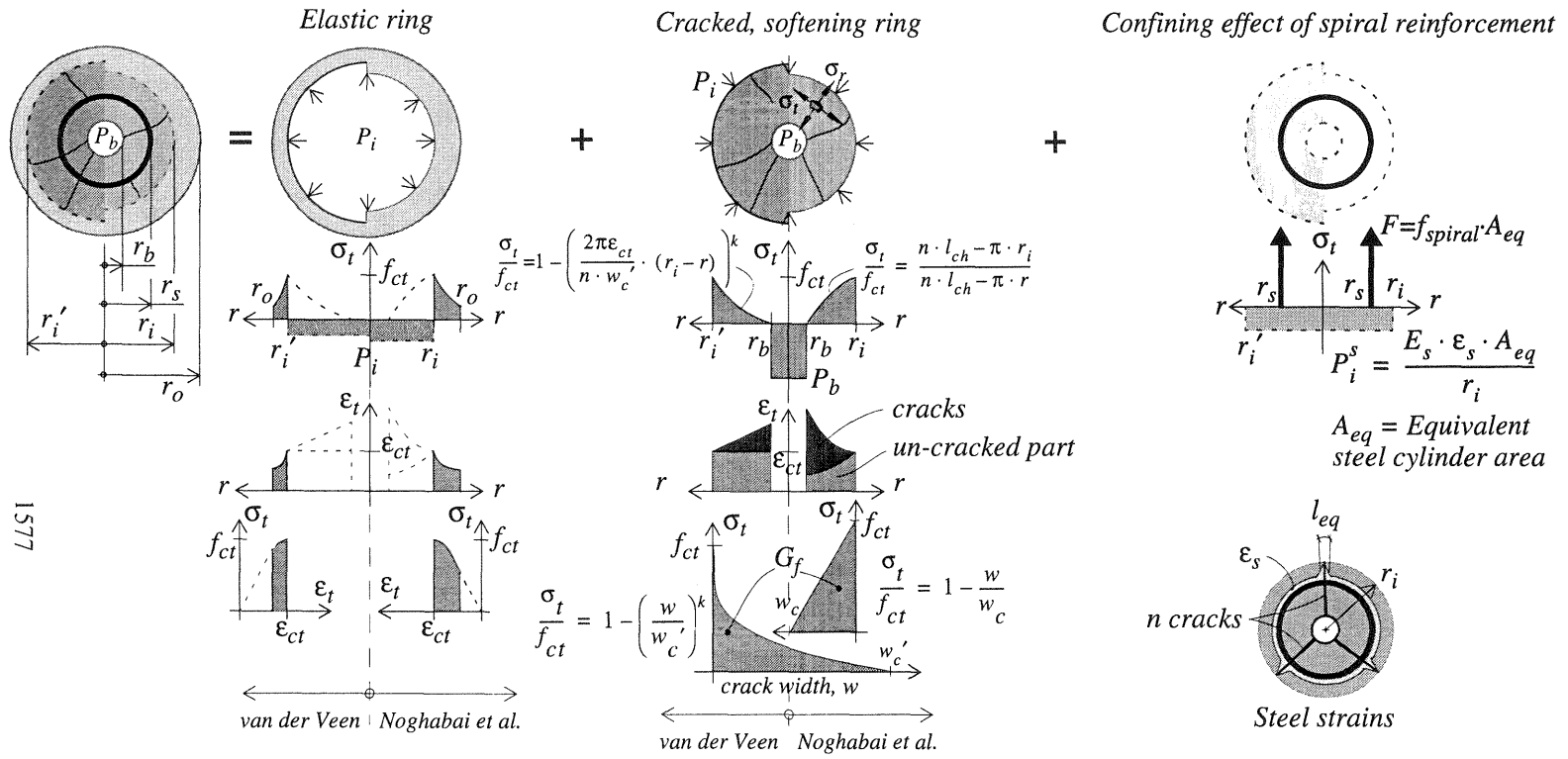
1 Introduction

Considering the practical limitation on the concrete cover, the problem of splitting constitutes an important restriction on for instance the ultimate bond capacity of reinforced concrete structures. The splitting phenomenon

is also dangerous, as it manifests a very brittle behaviour. This is accentuated when concrete of high strength is utilized. Theoretical splitting models have been deduced based on NLFM, which also take into account the confining effect of spiral reinforcement. The models are here verified by a so-called *membrane splitting test*, where concrete rings of different mixtures are subjected to an inner hydrostatic pressure until collapse. In order to investigate the correctness of the assumptions of the theoretical models and to acquire insight in the fracturing behaviour of a ring subjected to inner pressure, FE-analysis have also been carried out. Three different approaches have been used: The discrete crack approach, the smeared crack approach and the inner softening band approach, see Klisinski et al. (1995).

2 Theory - Splitting models

Tepfers (1973) adopted a limit analysis to the splitting failure of concrete covers for assessing the bar-to-concrete bonding capacity. However, it was proved experimentally (see e.g. Reinhardt, 1992 and Rosati et al., 1992), that the *strength* criteria alone is not sufficient for an accurate prediction. An additional energy criterion is required, incorporating the cohesive qualities of cracks due to aggregate interlocking *after* the strength limits are reached. To describe such post-peak, tensile (softening) material behaviour of concrete, Hillerborg et al. (1976) introduced NLFM in research on cementitious materials by proposing a constitutive law based on the *stress - crack opening displacement* (COD) relation along a so-called *fictitious* crack. Reinhardt (1992), Van der Veen (1990), Rosati et al. (1992) and Noghabai et al. (1993) incorporated the fictitious crack model in the partly-cracked-elastic-ring concept established by Tepfers (1973), each of them assuming an appropriate constitutive law that governs the softening. Hence, the concrete ring is considered to consist of one intact, elastic outer ring and one cracked, *softening* inner ring with a hydraulic pressure, P_b , acting on the circumference of the inner hole, see Fig. 1. With sufficient concrete cover, the ultimate pressure will be reached for a critical crack depth, r_i . Here we will only compare the models of van der Veen (1990) and Noghabai (1993, 1995). The general features of these two models are presented in Fig. 1. Due to lack of sufficient data, the exponent k in van der Veen's model will be set to 0.248 and the critical stress-free crack width $w_c = 5.14 \cdot G_f / f_{ct}$ for all cases, admitting the fact that this is only validated for a normal strength concrete.



Noghabai et al.
(1993, 1995):

$$\frac{P_b}{f_{ct}} = \frac{r_i}{r_b} \cdot \left(\frac{r_o^2 - r_i^2}{r_o^2 + r_i^2} \right) + \frac{n \cdot l_{ch} - \pi \cdot r_i}{\pi \cdot r_b} \cdot \ln \left(\frac{n \cdot l_{ch} - \pi \cdot r_b}{n \cdot l_{ch} - \pi \cdot r_i} \right) + \frac{E_s \cdot A_{eq}}{r_s \cdot E_c} \cdot \left[1 + \frac{l_{ch} \cdot (r_s - r_i) \cdot (2 \cdot \pi \cdot r_s - n \cdot l_{eq})}{l_{eq} \cdot r_i \cdot (\pi \cdot r_s - n \cdot l_{ch})} \right]$$

van der Veen
(1990):

$$\frac{P_b}{f_{ct}} = \frac{r'_i}{r_b} \cdot \left(\frac{r_o^2 - r'^2_i}{r_o^2 + r'^2_i} \right) + \frac{(r'_i - r_b)}{r_b} \cdot \left(1 - \frac{2\pi \cdot (r'_i - r_b)}{5.14 \cdot n \cdot l_{ch}} \right)^k \cdot \frac{1}{1+k} + \frac{E_s \cdot A_{eq}}{r_s \cdot E_c} \cdot \left[1 + \frac{(2 \cdot \pi \cdot r_s - n \cdot l_{eq}) \cdot (r'_i - r_s)}{r'_i \cdot l_{eq}} \right]$$

Fig. 1. General features of two splitting models, derived from Noghabai (1995)

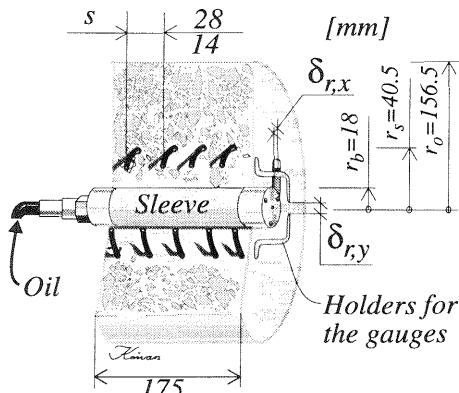
3 Experiment - membrane splitting tests

The specimens measured as in Fig. 2. Concentric holes were drilled out of the cylinders after the concrete had cured. Three batches of different concrete mixtures were used according to the table in Fig. 2. From each batch three cylinders were produced: A reference specimen (no spiral reinforcement) and two test pieces including spiral reinforcement made of $\phi 6$ mm deformed bar (Ks400, $E_s=210$ GPa), with the same radius, r_s , but with different pitches, s (28 and 14 mm, hence $A_{eq}=0.00101$ and $0.00202 \text{ m}^2/\text{m}$).

The compressive and tensile splitting strengths, f_{cc} and f_{csp} , were measured on concrete cubes, 150 mm for the NSC and HSC concrete and 100 mm cubes for the VHSC concrete. The fracture energy, G_f , were determined on notched beams with the dimension $840 \times 100 \times 100 \text{ mm}^3$. All specimens were submerged in water for at least 28 days after pouring.

The device with which the inner pressure was exerted to the cylinder (*membrane* or *sleeve*) consisted of a steel mandrel coated with a 2-3 mm thick membrane of polyurethane elastomer. Oil was pumped in the cavity between the mandrel and the inner membrane wall using a pressure controlled hydraulic pump (hence, the experiment was conducted in load-control). The radial displacement was measured in two orthogonal directions, symmetrically over the hole.

The material parameters of the concrete were determined in conjunction with the performance of the experiment and are summarized in Table 1.



Component	NSC	HSC	VHSC
Coarse aggregate	818	1149	1060
Fine aggregate	980	770	750
Cement	343	450	540
Silica fume	-	70	54
Superplastisizer	-	6.3	8.7
w/c	0.56	0.35	0.25

Fig. 2. The features of the test specimen. The table shows the concrete recipes (dry material [kg/m^3]) used in the splitting tests, denominated as: Normal Strength Concrete, NSC, High Strength Concrete, HSC and Very High Strength Concrete, VHSC. Expected 28-days compressive strengths (of cubic specimens) are 40, 80 and 140 MPa.

Table 1: Material parameters of the different concrete mixtures. The values in the parenthesis denotes days after pouring.

Parameters	NSC	HSC	VHSC	Notes
f_{cc}^{cube} [MPa]	57.0 (40)	105.0 (49)	157.4 (51)	Mean values of 6 cubes for the strengths and 6 RILEM beams for the fracture energy, tested shortly after the splitting test.
f_{cspl}^{cube} [MPa]	4.2 (40)	5.6 (49)	8.9 (51)	
G_f [Nm/m]	105 (40)	145 (57)	172 (53)	
E_c [GPa]	33.8 (74) 33.0 (40)*	39.4 (49)	41.2 (51)	Analytically derived except for NSC.
f_{ct} [MPa]	3.8	5.0	8.0	$0.9 \cdot f_{cspl}^{cube}$, according to Heilmann, see van der Veen (1990)
l_{ch} [m]	0.240	0.229	0.111	Characteristic length $l_{ch} = E_c \cdot G_f / f_{ct}^2$

*. Re-evaluated value to age corresponding to the time of testing, according to CEB-FIB model code 1990.

The following comments can be made on the behaviour (cf. Fig. 4 and 5):

- Stronger and more brittle concretes give smaller relative capacity, with respect to the f_{cc}, f_{cspl} or l_{ch} .
- NSC is more pronouncedly affected by the use of spiral reinforcement, but seems to be less sensitive towards the pitch density.
- A higher pitch density does not lead to a proportionally increase in the splitting capacity of the specimens.
- No premonition of failure was perceived in any case. At a certain limit the pressure gets too high and a single crack penetrates the concrete cover and provide enough space for other cracks to become visible. Thus, the state and distribution of the stresses the cylindrical specimens provide, influences the formation of the cracks *disregarded* the strength of the concrete and *ergo* must be a key issue.
- It is doubtful whether such experiments could be conducted in displacement control.
- Spiral reinforcement probably only affects the peak capacity of a specimen and not its overall stiffness, which is destined as soon as cracks are triggered (σ_t exceed the f_{ct}) and are not initially affected by the spiral.

4 Numerical simulations - different FEM approaches

The geometry of the specimens defined in Fig. 2 has been modelled with different meshes for FEM simulations. The modelling strategy for the different approaches are shown in Fig. 3. To simulate the material imperfections for the discrete crack approach, the crack initiation threshold (f_{ct}) for the interfaces were alternately over- and underestimated by 5% (denoted by + and - in Fig. 3). The complete ring as well as the semi-ring were analysed in the discrete and smeared crack approaches. It was noted that the discrete analysis was almost insensitive towards the choice of geometrical model due to a “smearing-out” of the fracturing behaviour, whereas the results of the smeared analysis were profoundly inflicted by any use of the symmetry in the geometry. Based on this experience only the whole of the ring was analysed with the ISB approach. Poisson’s ratio was set to zero (based on the theory) and plain strain elements were used in all cases. The pressure was simulated by a successive increase of the nodal forces on the perimeter of the hole.

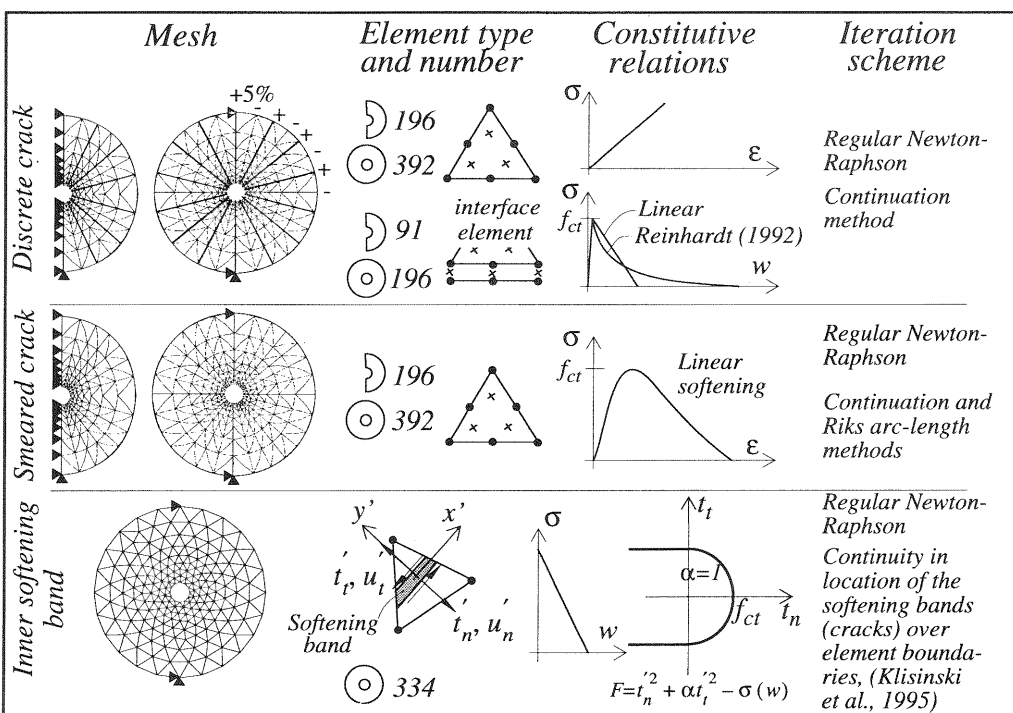


Fig. 3. FEM approaches employed in the analysis.

5 Comparison between theory, experiments and FE-analysis

Fig. 4 to 6 show different comparisons between the theoretical models, the experiments and the FE-analysis.

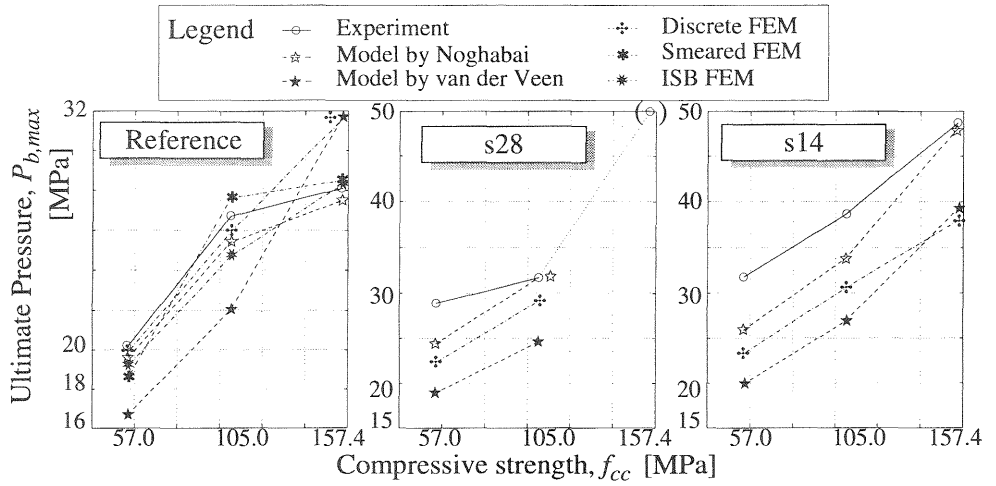


Fig. 4. Comparison of the ultimate capacity for the different concretes, obtained from experiments, theoretical models and FEM. VHSCs28 is not to be relied (within parenthesis).

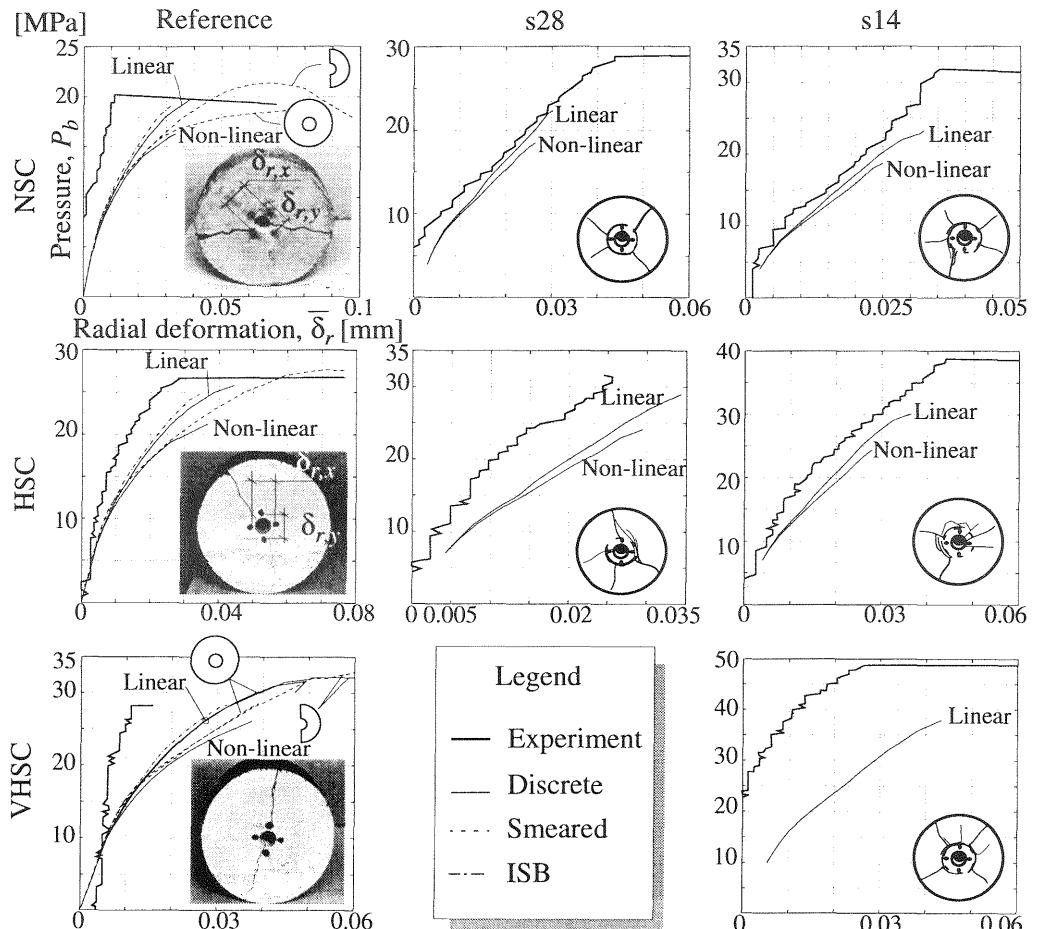


Fig. 5. Comparison between the experimental and FEM results. The inlaid illustrations and photos show the fractured state of the specimens.

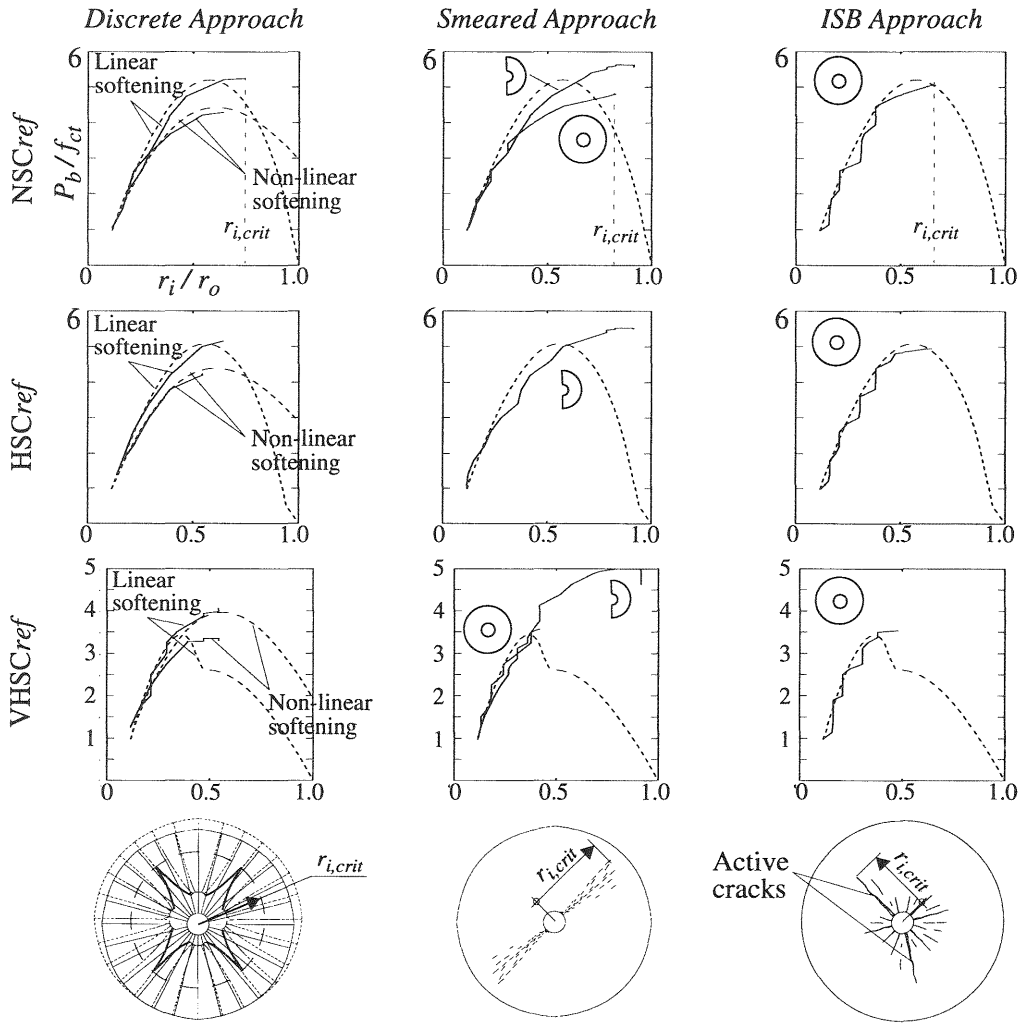


Fig. 6. Comparison between the theoretical models (dashed) and the FEM-analysis (full lines). The figures at the bottom show a typical fracturing situation for each approach at ultimate pressure (P_b at $r_{i,crit}$).

It is thus proved that the model of Noghabai et al. (1993) gives less discrepancy from the experimental results than the model of van der Veen (1990), see Fig. 4. Also, the FE-analysis affirms that a linear softening gives less discrepancy (Fig. 4-6). The tension stiffening effect for all spiral reinforced cases is almost neglected ($n \cdot l_{eq} \rightarrow 2 \cdot \pi \cdot r_s$ in the equations of Fig. 1), which might explain the increase in error for such cases.

An overall comparison between FE-models and experimental results indicates that the ISB approach exhibits the most consistent behaviour of the models (also cf. the “ISB-ring” in Fig. 6 with the authentic cases shown

by photographs in Fig. 5). In this context, the theoretical models should be considered as approximations to the very plausible description of the fracturing behaviour of a concrete ring the FE-models offer, see Fig. 6.

6 Discussion

The differences between the models of Noghabai and van der Veen become perhaps more evident by making use of the brittleness number, B . In Fig. 7, the ultimate (relative) pressure for different B are plotted in logarithmic scales. This is done for the reference cases (no spiral), wherefore the number of cracks, n , is set to two. The logarithmic expression of Noghabai, see Fig. 1, (which is in fact due to the strain assumptions in the cracked part) subdues the contribution of the softening ring for more brittle concretes, which is both plausible and harmonizes with the experiments.

Quintessential for this problem (and specimens of this size and shape) seem to be crack stability and the role the gradients of the assumed softening curves might play, without offering further proof.

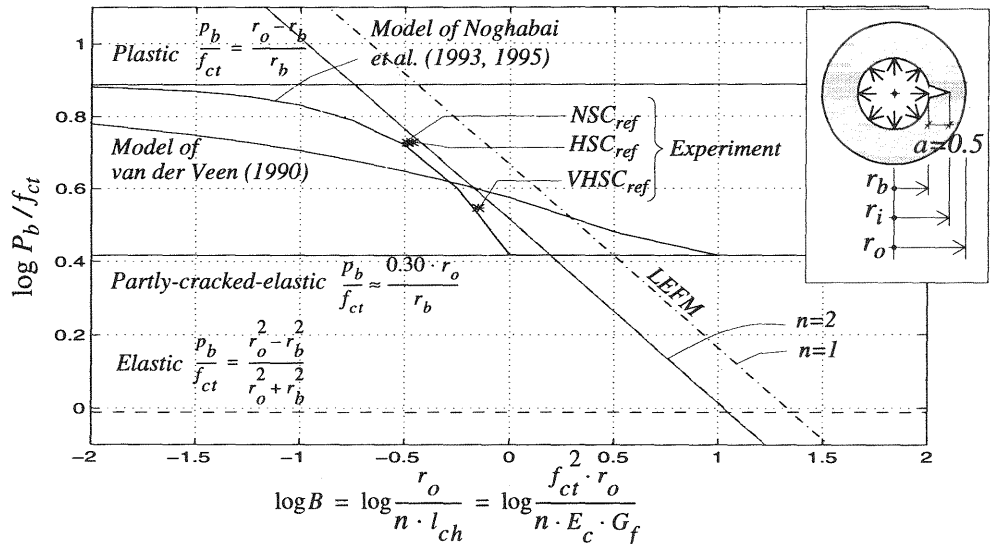


Fig. 7. The ultimate relative pressure given by the different models for a concrete ring ($r_b=18$ and $r_o=156.5$ mm) as a function of B , in log scale. A linear elastic fracture mechanics (LEFM) analysis based on Bowie et al. (1972), with one and two existing cracks (i.e. $n=1$ and 2) with an assumed crack length (a) of 0.5 mm, is also included. The horizontal lines indicated by “Plastic”, “Partly-cracked-elastic” and “Elastic” are according to the models of Tepfers (1973).

7 Conclusion

A very good correspondence was achieved between experimental results and the analytical model proposed by Noghabai (1993, 1995). The proposed

model gives a correct description of the brittleness of the splitting failure when applied to high strength concrete. The results are also verified by means of FEM, where the analysis based on the inner softening band concept was proved to give the most consistent results, compared to the discrete crack and smeared crack approaches.

8 Acknowledgement

The work was supported by "Axel och Margaret Ax:son Johnsons Stiftelse" and the Swedish Council for Building Research. The work was supervised by Prof. Lennart Elfgeren and Dr. Thomas Olofsson.

9 References

- Bowie, O.L. and Freese, C.E. (1972) Elastic analysis for a radial crack in a circular ring, **Engineering Fracture Mechanics**, vol. 4, 315-321.
- Hillerborg, A., Modeer, M. and Petersson, P-E. (1976) Analysis of crack formation and crack growth in concrete by means of fracture mechanics and finite elements, **Cement and Concrete Research**, vol. 6, 773-782.
- Klisinski, M., Olofsson, T. and Tano, R. (1995) Mixed mode cracking of concrete modelled by inner softening band, **Computational Plasticity** (eds D.R.J Owen, E. Oñate and E. Hinton), Barcelona, part 2, 1595-1606.
- Noghabai, K., Olofsson, T. and Ohlsson, U. (1993) Bond properties of high strength concrete, **Utilization of High-Strength Concrete** (eds I. Holand and E. Sellevold), Lillehammer, Norway, 1169-1176.
- Noghabai, K. (1995) **Splitting of Concrete in the Anchoring Zone of Deformed Bars - A Fracture Mechanics Approach**, Licentiate Thesis, Luleå University of Technology, Luleå, Sweden. To be published.
- Reinhardt, H.W. (1992) Bond of steel to strain-softening concrete taking account of loading rate. **Fracture Mechanics of Concrete Structures** (ed Z. Bazant), Elsevier, London, 809-820.
- Rosati, G. and Schumm, C. (1992) Modelling of local bar-to-concrete bond in reinforced concrete beams. **Bond in Concrete - From Research to Practice** (eds A. Skudra and R. Tepfers), Riga, Latvia, vol. 3, 12:34-43.
- Tepfers, R. (1973) **A Theory of Bond Applied to Overlapped Tensile Reinforcement Splices for Deformed Bar**. Dissertation, Chalmers University of Technology, Göteborg, Sweden, 1973.
- van der Veen, C. (1990) **Cryogenic Bond Stress-Slip Relationship**. Doctoral thesis, Delft University of Technology, Delft, The Netherlands.